Time-Resolved Photointermediate Changes in Rhodopsin Glutamic Acid 181 Mutants†

James W. Lewis,‡ Istvan Szundi,‡ Manija A. Kazmi,§ Thomas P. Sakmar,§ and David S. Kliger*,‡

Department of Chemistry and Biochemistry, University of California, Santa Cruz, Santa Cruz, California 95064, and Howard Hughes Medical Institute and Laboratory of Molecular Biology and Biochemistry, Rockefeller University, 1230 York Avenue, New York, New York 10021

Received March 1, 2004; Revised Manuscript Received May 12, 2004

ABSTRACT: The role of glutamic acid 181 in the bovine rhodopsin retinylidene chromophore pocket was studied by expressing E181 mutants in COS cells and measuring, as a function of time, the absorbance changes produced after excitation of lauryl maltoside pigment suspensions with 7 ns laser pulses. All mutants studied except E181D showed accelerated decay of bathorhodopsin compared to wild type. Even for E181D, an anomalously large blue shift was observed in the absorption spectrum of the bathorhodopsin decay product, BSI. These observations support the idea that E181 plays a significant role in the earliest stages of receptor activation. E181 mutations have a pronounced effect on the decay of the lumirhodopsin photointermediate, primarily affecting the size of the red shift that occurs in the lumirhodopsin I to lumirhodopsin II transition that takes place on the 10 μs time scale after wild-type photoexcitation. While the spectral change that occurs in the lumirhodopsin I to lumirhodopsin II transition in wild-type rhodopsin is very small (∼2 nm), making it difficult to detect, it is larger in E181D (∼6 nm), making it evident even in the lower signal-to-noise ratio measurements possible with rhodopsin mutants. The change seen is even larger for the E181F mutant where significant amounts of a deprotonated Schiff base intermediate are produced with the 10 μs time constant of lumirhodopsin II formation. The E181Q mutant shows lumirhodopsin decay more similar to wild-type behavior, and no lumirhodopsin I to lumirhodopsin II transition can be resolved. The addition of chloride ion to E181Q increases the lumirhodopsin I−lumirhodopsin II spectral shift and slows the deprotonation of the Schiff base. The latter result is consistent with the idea that a negative charge at position 181 contributes to protonated Schiff base stability in the later intermediates.

Our ability to see visible light depends largely on the fact that the retinal chromophore in rhodopsin, our scotopic visual pigment, occurs as a protonated Schiff base (PSB)[1] with Glu113 as its counterion. The corresponding counterion for invertebrate rhodopsins long eluded discovery, but recently it was shown that in cephalopod retinochrome, a member of the rhodopsin family, the counterion corresponds to vertebrate rhodopsin residue E181 (*1*). Mutation of that amino acid in bovine rhodopsin was shown to affect the pigment spectrum, and the X-ray crystal structure of rhodopsin (published while the retinochrome work was in press) shows that E181 indeed lies close to the chromophore (*2*). The inference that the residue corresponding to rhodopsin E181 can serve as the counterion for invertebrate visual pigments has recently been confirmed (*3*). The presence of a second ionizable group in the hydrophobic retinylidene chromophore binding pocket, in a position that is known to act as the counterion for an all-*trans*-retinylidene PSB in at least one rhodopsin family member, is a tantalizing coincidence for those interested in the vertebrate rhodopsin activation mechanism. Recent static preresonance Raman data on the E181Q mutant show little perturbation of the WT 1655 cm^{-1} C═N stretching mode, which has been interpreted to mean that E181 is neutral in the dark but becomes a titratable counterion at the metarhodopsin I stage (*4*). Previous time-resolved resonance Raman spectra of bovine rhodopsin have shown the PSB changes its hydrogen-bonding environment early in the activation process (*5*). Since at least two PSB intermediates can occur after this hydrogen-bonding change, transient absorbance measurements were conducted with E181 mutants to elucidate the role of the second pocket carboxylic acid side chain.

MATERIALS AND METHODS

Preparation of Rhodopsin Mutants. Site-directed mutagenesis of bovine opsin was carried out as previously reported (*6*). Opsin genes were expressed in COS-1 cells, and the product protein was regenerated with 11-*cis*-retinal. The resulting pigment was purified and concentrated as described previously (*7*, *8*). Samples for transient absorbance measure-

† This work was supported by Grant EY00983 from the National Eye Institute of the National Institutes of Health (to D.S.K.) and the Allene Reuss Memorial Trust. T.P.S. is an Associate Investigator of the Howard Hughes Medical Institute.

* To whom correspondence should be addressed. Telephone: (831) 459-2106. Fax: (831) 459-4136. E-mail: kliger@chemistry.ucsc.edu.

‡ University of California, Santa Cruz.

§ Rockefeller University.

[1] Abbreviations: Batho, bathorhodopsin; BSI, blue-shifted intermediate; LM, lauryl maltoside; Lumi, lumirhodopsin; Meta, metarhodopsin; PSB, protonated Schiff base; WT, wild type.

10.1021/bi049581l CCC: $27.50
Published on Web 09/04/2004

ments were solubilized in 0.1% dodecyl maltoside and 0.5 mM phosphate buffer, pH 7.0, without added chloride except where specifically noted. Typically ~150 μg of pigment was used to collect the data shown in Figures 1 and 2. As a control to show that the changes seen here are specific to E181 mutations and are not general to all extracellular loop II mutants, M183L and H195A were prepared, and similar time-resolved measurements were made.

Time-Resolved Spectroscopy. Individual 1 μL samples were photolyzed by 7 ns (fwhm) laser pulses. The change in the absorption spectrum at a particular time delay after photolysis, ranging from 30 ns to 690 ms, was measured using a gated optical multichannel analyzer (*9*). In most cases samples were excited using 477 nm light from a dye laser pumped by the 355 nm third harmonic of a Nd:YAG laser since this avoids photolysis of bathorhodopsin, the intermediate usually present during the photolysis pulse. For E181F, measurements were also made using 532 nm excitation with the second harmonic of the Nd:YAG laser in order to determine whether photolysis of a blue-shifted early product occurred to a significant extent. In both cases the energy delivered to the sample was 100 μJ/mm^2. Absorbance changes were monitored using a flashlamp producing white probe light that was polarized at 54.7° relative to the laser polarization direction in order to minimize kinetic artifacts due to rotational diffusion. The path length of the probe light in the sample was 2 mm, typical pigment concentrations were ~0.5 mg/mL, and the sample temperature was maintained at 20 °C.

Data Analysis. The set of experimental difference spectra, $\{\Delta A(\lambda,t)\}$, were fit as described previously (*10*) to a function whose form was a sum of exponential decays:

$$\Delta a(\lambda,t) \equiv b_0(\lambda) + b_1(\lambda)\exp(-t/\tau_1) + b_2(\lambda)\exp(-t/\tau_2) + \ldots$$

The apparent lifetimes, τ_i, and the difference spectra, or b-spectra, $b_i(\lambda)$, associated with the individual lifetimes are unambiguously determined by the fitting process. If one photointermediate completely transforms into another in an exponential process, and it is well isolated in time from other processes, then the b-spectrum associated with the isolated process can be simply interpreted as the difference between the spectra of the two intermediates. However, in general a b-spectrum must be decomposed into multiple intermediate spectra consistent with the chemical mechanism (which must be determined). A procedure for finding the mechanism and determining spectra of photointermediates was described previously (*11*).

RESULTS

Absorbance difference spectra collected at time delays from 30 to 600 ns following laser excitation of E181 mutants are shown in Figure 1. Data were collected at only a few delay times in this region because of limitations on the amounts of rhodopsin mutants available and because it was presumed that E181's most interesting role begins after the PSB has broken away from its original hydrogen bond acceptor at the lumirhodopsin stage (*5*). The early E181D data shown in Figure 1a display the most similarity to wild-type rhodopsin. At 20 °C three rhodopsin photointermediates

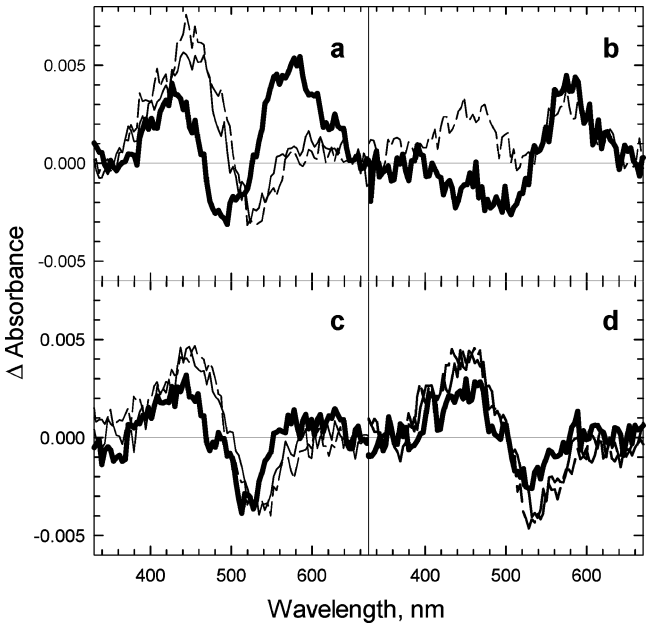

FIGURE 1: Early time-resolved absorbance changes observed after photoexcitation of rhodopsin E181 mutants. Heavy lines show the absorbance changes observed at 30 ns, light lines show the change at 200 ns, and the broken lines show the changes observed 600 ns after excitation with a 7 ns pulse of 477 nm light. (a) shows the data obtained from the E181D mutant. These data are qualitatively similar to what is observed after wild-type rhodopsin photolysis under these conditions. The transient absorbance peak near 560 nm is due to Batho, which decays into an equilibrium with BSI from 30 to 200 ns. Subsequently, from 200 to 600 ns, this equilibrated mixture decays to Lumi I. (b) shows the data for E181F. For E181F little change is seen in the red portion of the spectrum, suggesting that Batho has decayed within 30 ns into equilibrium with BSI. Changes seen in the blue portion of the spectrum for E181F are consistent with decay of BSI to Lumi I. (c) shows data from E181Q with 200 mM chloride ion. (d) shows data for E181Q without added chloride. The data in all panels have been scaled to have the same amplitude pigment bleach.

appear on the submicrosecond time scale and follow the scheme (*10*):

$$\ldots \underset{529\ \text{nm}}{\text{Batho}} \overset{40\ \text{ns}}{\rightleftharpoons} \underset{477\ \text{nm}}{\text{BSI}} \xrightarrow{200\ \text{ns}} \underset{490\ \text{nm}}{\text{Lumi}} \ldots$$

The positive transient absorption that appears in the red portion of the 30 ns difference spectrum and decays away within 200 ns suggests that E181D bathorhodopsin (Batho) has stability similar to wild-type Batho. For the other E181 mutants shown in Figure 1, Batho is apparently less stable and has decayed into equilibrium with the blue-shifted intermediate (BSI) prior to data collection at 30 ns. Thus, in E181Q and E181F absorbance changes from 30 to 600 ns report the decays of the Batho−BSI equilibrated mixture to lumirhodopsin (Lumi). Lifetimes observed for the changes seen on the early time scale are given in Table 1. An estimate of the composition of the equilibrated mixture of Batho and BSI was obtained by fitting the broad absorbance spectrum of the mixture observed at 30 ns as the sum of a Batho, red shifted by 29 nm from the pigment spectrum, and a second absorber attributed to BSI. The λ_{max}'s of the resulting BSI's are given in Table 2, and the compositions estimated for the mixtures are given in Table 3. Due to the limited data collected at submicrosecond delay times, considerable uncertainty exists about the Batho/BSI ratio in the equilibrated

Table 1: Apparent Lifetimes Used in Fitting Time-Resolved Absorbance Changes

	τ_1/τ_2 (ns)	τ_3 (μs)	τ_4 (μs)	τ_5 (ms)
E181D	30−50/150−250	12	100	2.6
E181F	200[a]	10	80	2.1
E181QCl	170[a]	11	90	0.93[b]
E181Q	200[a]	*c*	85	1.0
rhodopsin	40/240[d]	12[e]	130[f]	1.25[f]

[a] Only a single exponential could be resolved on the time scale leading to lumirhodopsin formation. [b] On the basis of the change observed at only the two latest delay times, an additional component could be fit whose lifetime was 10 ms. [c] No component in this time range was needed to fit these data. [d] Hug et al. (*10*). [e] Szundi et al. (*14*). [f] For comparison, the two slowest lifetimes detected by Mah et al. in larger samples of LM-solubilized rhodopsin have been averaged (*27*).

Table 2: λ_{max} of Model Spectra Used in Fitting Time-Resolved Absorbance Changes

	bleach/ pigment	Batho	BSI	Lumi I	Lumi II	Meta I_{380}	Meta II
E181D	499/497	526	460	481	487	375	376
E181F	503/501	530	490	496	504/380[a]	370	372
E181QCl	508/505	534	485	491	494	376	379/376[b]
E181Q	513/508	537	492	493[c]	493[c]	381	381
rhodopsin	504/498	529[d]	477[e]	488.5[e]	490[e]	377[f]	377[f]

[a] This pigment formed an early 380 nm absorbing product after decay of Lumi I which was followed by a 370 nm absorbing intermediate which corresponds temporally to Meta I_{380}. [b] On the basis of data at only two delay times, a second form of Meta II may be present which forms with a time constant of 10 ms. [c] No spectral evolution on the Lumi I−Lumi II time scale was detected for this pigment; only a single 493 nm Lumi product was detected. [d] Jäger et al. (*28*). [e] Szundi et al. (*14*). [f] Mah et al. (*27*).

mixture and, where little Batho was present at 30 ns, about the Batho λ_{max} as well.

As can be seen in Figure 1b, after photoexcitation of E181F unusual positive transient absorbance appears at 30 ns in the red region that persists for at least 1 μs after excitation. Since substantial amounts of E181F BSI are present during the 477 nm laser pulse, and its photolysis could produce secondary photoproducts absorbing in the red, an experiment was conducted using a pulse of 532 nm light to excite E181F (data not shown). The results showed similar transient absorbance formation in the red as is seen in the 477 nm data in Figure 1. Signals were also somewhat smaller amplitude, indicating that photolysis of Batho is a more important pathway for photo-back-reaction than photolysis of BSI. A shift in the bleach observed for 532 nm excitation was consistent with somewhat more isopigment (9-*cis*) being formed, but otherwise data were similar to that seen in Figures 1b and 2b. Thus, since the E181F red transient absorbance is not photolabile and does not decay on the submicrosecond time scale, it is unlikely to be due to a Batho intermediate. Submicrosecond transient absorbance changes in the blue region of the E181F difference spectra support the idea that E181F Batho has decayed prior to 30 ns, leaving only a BSI to Lumi process in the 30 ns to 1 μs region.

Data collected after photoexcitation of E181Q (±chloride) are shown in Figure 1c,d. The absence of red transient absorbance at 30 ns in both cases indicates that Batho is destabilized by the E181Q mutation and has decayed into equilibrium with BSI prior to 30 ns. This behavior is similar to that of destabilized Batho intermediates observed after photoexcitation of many rhodopsins with artificial retinal chromophores (*12*) and of several rhodopsin mutants affecting the chromophore pocket (*13*).

Data for the E181 mutants on the time scale following that of Figure 1 are shown in Figure 2. Again, E181D shows the greatest similarity to what is observed after photolysis of bovine rhodopsin. Residuals from one-, two-, and three-exponential fits of the E181D data are shown in Figure 3. As shown there, E181D data are poorly fit by a single exponential, and flat residuals are not obtained from the best two-exponential fit, which adds a small slow component. However, as shown in Figure 3c, a three-exponential fit which contains a small 12 μs component yields residuals which are within the experimental noise present in the data. Support for the presence of a 12 μs component in the E181D data comes from the fact that a component with similar lifetime has recently been reported after bovine rhodopsin photolysis and has been associated with a Lumi I to Lumi II transition (*14*). Thus, the scheme which governs the later intermediates in detergent suspensions of bovine rhodopsin is

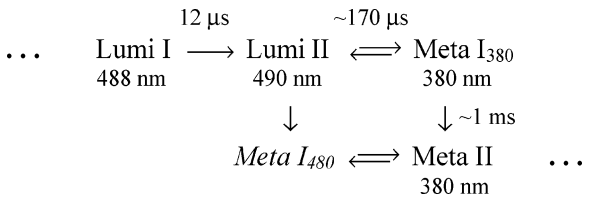

where Meta I_{480} is shown in italics because little or none appears at the high detergent to lipid ratios which prevail in the preparations studied here. The 12 μs spectral shift occurring in the E181D data is in the same direction as that seen for bovine rhodopsin, but as shown in Figure 4, the shift is somewhat larger than the bovine rhodopsin Lumi I−Lumi II shift. The lifetimes fit to the E181D data are given in Table 1. The λ_{max}'s of the sequential intermediates determined from fitting the E181D data are given in Table 2.

Comparison of the 100 μs curves in Figure 2a,b shows that the fast component is even more prominent in the E181F data. The inadequacy of a single-exponential fit to these data is demonstrated by the residuals presented in Figure 5. The third trace from the bottom in Figure 5 shows that flat residuals were obtained for the 30 μs difference spectrum, a delay time identical to the best single-exponential fit. The opposite curvature of the residuals at higher and lower delay times points to the need for both faster and slower components. Again for E181F a three-exponential fit was required to produce flat residuals, comparable to the lower set in Figure 3. In contrast to the case of E181D where the second intermediate (presumably pure Lumi II) shows only a small red shift from Lumi I, when the E181F data are analyzed in terms of a straight sequential scheme, the second intermediate as shown in Figure 6 appears to be a mixture containing a deprotonated Schiff base component, which we designate as Lumi II_{380}. The designation of an additional intermediate (besides Meta I_{380} and Meta II) is needed in this case because 380 nm absorbance develops in three clear phases. The time constants determined for E181F are given in Table 1, the λ_{max}'s of the sequential intermediates are given in Table 2,

Table 3: Composition of Sequential Intermediates Determined by Fitting Time-Resolved Absorbance Changes

	30 ns	intermediate 3	intermediate 4	intermediate 5	intermediate 6
E181D	0.55 Batho 0.45 BSI	Lumi I	Lumi II	0.15 Lumi II 0.85 Meta I_{380}	Meta II
E181F	0.3 Batho 0.7 BSI	Lumi I	0.4 Lumi II 0.6 Lumi II_{380}	0.05 Lumi II 0.95 Meta I_{380}	Meta II
E181QCl	0.3 Batho 0.7 BSI	Lumi I	Lumi II	0.27 Lumi II 0.73 Meta I_{380}	Meta II
E181Q	0.2 Batho 0.8 BSI	Lumi	*a*	0.15 Lumi 0.85 Meta I_{380}	Meta II
rhodopsin	0.7 Batho[b] 0.3 BSI	Lumi I	Lumi II	0.3 Lumi II[c] 0.7 Meta I_{380}	Meta II

[a] No sequential intermediate was found on the time scale of the intermediate 4 found after photoexcitation of other pigments. [b] Hug et al. (*10*). [c] Szundi et al. (*29*).

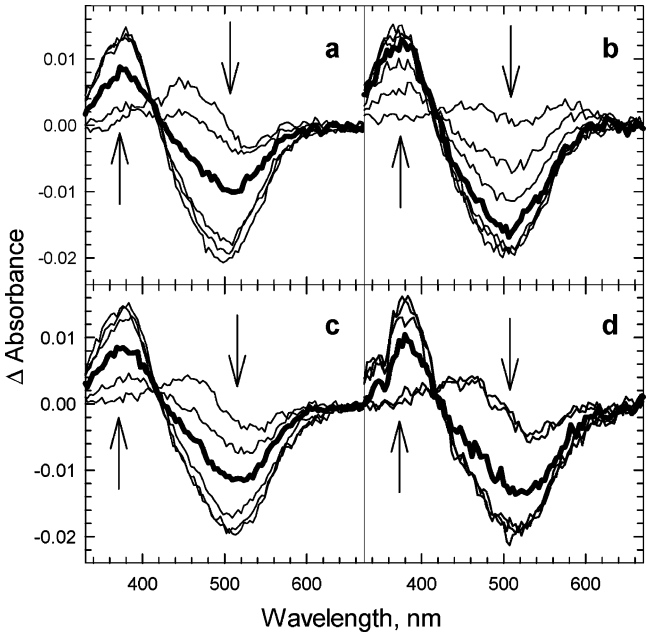

FIGURE 2: Later time-resolved absorbance changes observed after photoexcitation of rhodopsin E181 mutants. These absorbance difference spectra are a continuation of the changes seen in Figure 1. The top curve shown in each panel corresponds to the 600 ns data from Figure 1, and arrows indicate the direction of absorbance changes at increasing times. In all panels, the heavy line shows data at 100 μs after photoexcitation. In all cases, the time delays for the last three curves are 500 μs, 2 ms, and 690 ms. Additional curves are as follows: (a, E181D) 30 μs, (b, E181F) 10 and 30 μs, (c, E181Q with 200 mM chloride) 30 μs, and (d, E181Q without chloride) 3.6 μs.

and the compositions of mixtures estimated from decomposing the spectra are given in Table 3.

Absorbance difference spectra for E181Q containing 200 mM chloride ion also required at least three exponential processes for an adequate fit. The first three had characteristics generally similar to those seen in E181D and wild-type rhodopsin (i.e., no very early deprotonation of the Schiff base). When analyzed in terms of a straight sequential scheme, the intermediates shown in Figure 7 were obtained (time constants are given in Table 1, λ_{max}'s of the sequential intermediates are given in Table 2, and the compositions of mixtures estimated from decomposing the spectra are given in Table 3). In addition to these, a very slow process ($\tau \sim$ 10 ms) may have been present, but its lifetime and even its presence are uncertain because it represents a small change between data collected at only two delay times. Because this process would correspond to an ~3 nm blue shift of an intermediate absorbing near 380 nm, it does not affect a very large portion of the spectral region studied here, and hence

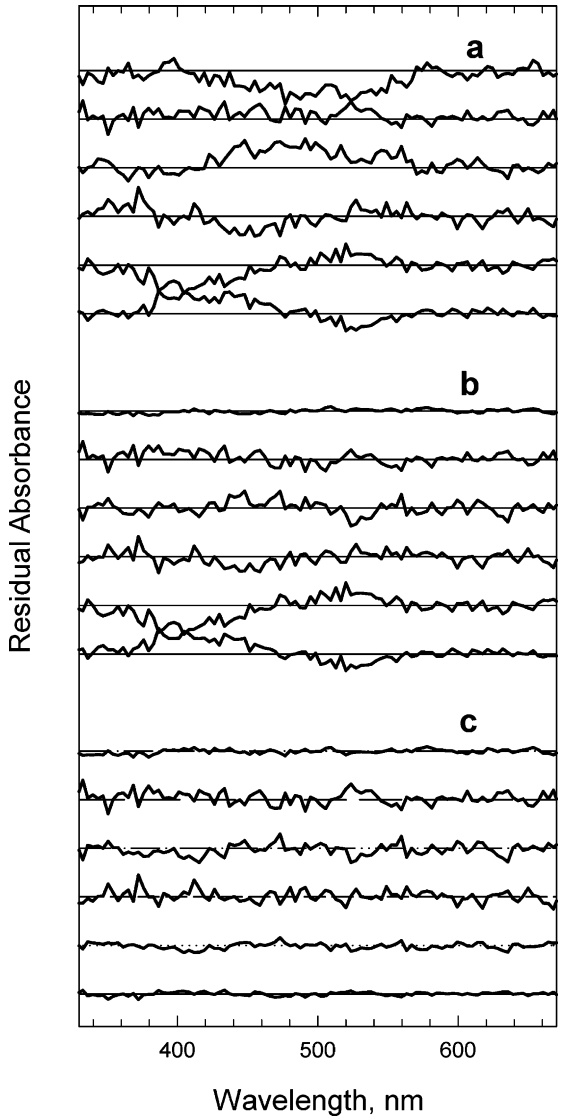

FIGURE 3: Residuals from one-, two-, and three-exponential fits of the E181D data in Figure 2. (a) Residuals from the best single-exponential fit, 140 μs. The earliest time (600 ns) is at the bottom. (b) Residuals from the best two-exponential fit, 120 μs and 3.8 ms. The low noise level in the 690 ms residual results from the noise present in that data being included in the b-spectrum of the slowest component. (c) Residuals from the best three-exponential fit, 12 μs, 100 μs, and 2.6 ms. As was the case in (b), when a slow component appeared, the presence of a fast component reduces the residuals at early times.

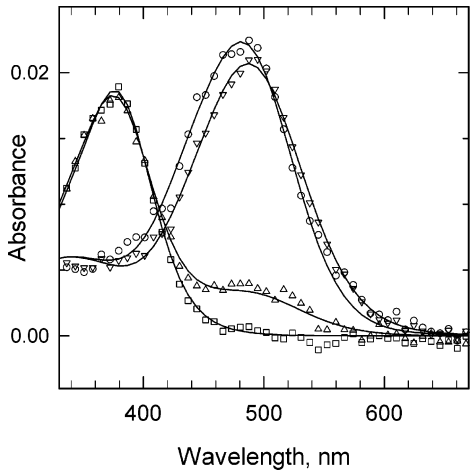

FIGURE 4: Spectra of E181D sequential intermediates. Symbols show the spectra obtained by fitting the data to a straight sequential mechanism (A → B → C → D). Smooth curves show the best fit to these sequential intermediate spectra (which can represent equilibrated mixtures) using the model pure intermediate spectra described in Table 2. Key: (○) Lumi I, (▽) Lumi II, (△) 0.15 Lumi II and 0.85 Meta I_{380}, and (□) Meta II.

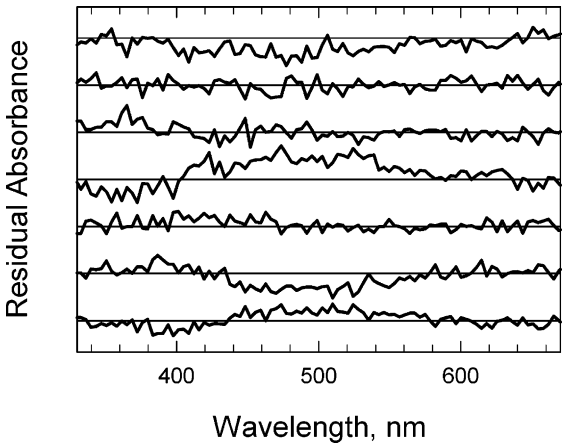

FIGURE 5: Residuals from a single-exponential fit to the E181F data from Figure 2. The best single-exponential fit, 30 μs, yields poor residuals. Data collected using 532 nm excitation had similarly shaped, poor residuals. The fit using two exponentials was also poor, but the three-exponential fit yielded flat residuals comparable to those in Figure 3c.

its characteristics are correspondingly less certain. In contrast to the presence of the possible extra process found in the data for E181Q with added chloride, the data for E181Q without added chloride were fit adequately using only two exponentials. Those two correspond to the formation and decay of Meta I_{380}, so the transition from Lumi I to Lumi II was not resolved. However, it could still be present with a small shift similar to what is seen in wild-type rhodopsin since at the signal-to-noise ratio and sparse delay time values obtainable with small amounts of mutant pigments it is doubtful if a shift of the magnitude of wild-type Lumi I to Lumi II could be resolved. It does seem likely that any Lumi I−Lumi II spectral shift in E181Q without chloride is smaller than the shift observed for E181D, E181F, or E181Q with chloride. The spectra of the straight sequential intermediates found for E181Q with chloride are shown in Figure 8. Note that the spectra of these sequential intermediates vary more between the various E181 mutants than do the lifetimes of the processes involved in their

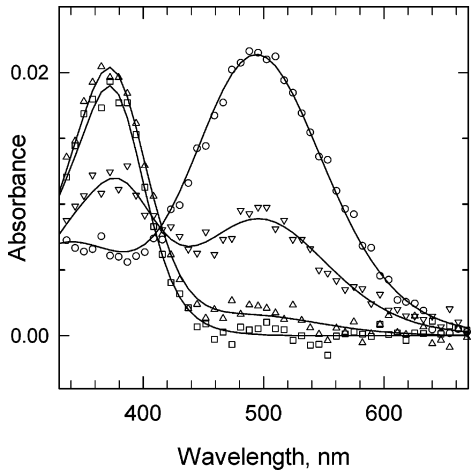

FIGURE 6: Spectra of E181F sequential intermediates. Symbols show the spectra obtained by fitting the data to a straight sequential mechanism. Smooth curves show the best fit to these sequential intermediates using the model pure intermediate spectra described in Table 2. Key: (○) Lumi I, (▽) 0.4 Lumi II and 0.6 Lumi II_{380}, (△) 0.07 Lumi II and 0.93 Meta I_{380}, and (□) Meta II.

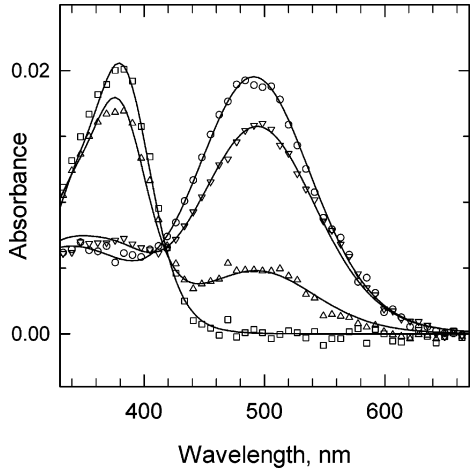

FIGURE 7: Spectra of E181Q + chloride sequential intermediates. Symbols show the spectra obtained by fitting the data to a straight sequential mechanism. Smooth curves show the best fit to these sequential intermediates using the model pure intermediate spectra described in Table 2. Key: (○) Lumi I, (▽) Lumi II, (△) 0.27 Lumi II and 0.73 Meta I_{380}, and (□) Meta II. On the basis of a change seen between data at the last two time delays for this pigment, there may be a further shift to 376 nm at very late times not shown in these intermediate spectra.

formation. Hence the composition of these mixtures in terms of "pure" intermediates (given in Table 3) tells more about the stability of the PSB than do the time constants given in Table 2.

Results for the two control mutations in extracellular loop II, M183L and H195A (data not shown), were not significantly different from those for wild-type rhodopsin expressed in COS cells. Normal stability of Batho was observed in both cases, and no definite detection of any Lumi I−Lumi II shift was possible with the amounts of pigment used here (as would be the case for wild-type rhodopsin with <200 μg of pigment). Single-exponential fits of data comparable to those in Figure 2 for the control mutants yielded time constants (200 μs for M183L and 260 μs for H195A) that were longer than any seen for the E181 mutants studied here, but which were in the range expected for wild-type preparations.

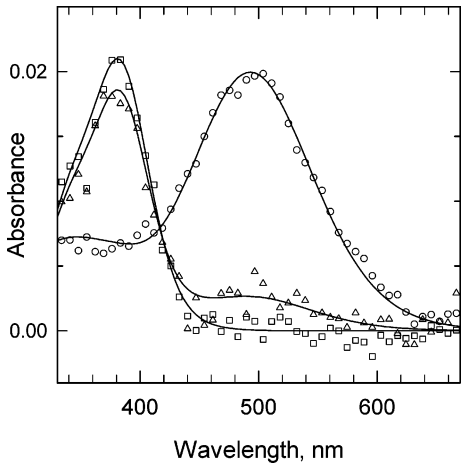

FIGURE 8: Spectra of E181Q sequential intermediates without chloride. Symbols show the spectra obtained by fitting the data to a straight sequential mechanism. Smooth curves show the best fit to these sequential intermediates using the model pure intermediate spectra described in Table 2. Key: (○) Lumi, (△) 0.13 Lumi and 0.87 Meta I_{380}, and (□) Meta II.

DISCUSSION

Recent developments have greatly increased interest in the function of glutamic acid 181 in vertebrate rhodopsins. The presence of another glutamic acid in the chromophore binding pocket besides the Schiff base counterion at 113 raises the possibility of a counterion shift at some point in the activation sequence and has recently been proposed to explain pH effects on E181Q's metarhodopsin I−metarhodopsin II equilibrium (*4*). Such a hypothesis invites study of rhodopsin 181 mutants using time-resolved absorbance measurements. However, while such studies are clearly relevant to this question, their interpretation depends on detailed understanding of the role of other structural elements revealed by X-ray studies in the vicinity of extracellular loop II which separates the chromophore from the intradiscal aqueous phase, an understanding which is in its early stages of development. Unlike FTIR and resonance Raman which at least in principle can directly reveal protonation states of amino acid side chains, optical absorbance spectra report directly only the protonation state of the retinylidene Schiff base, leaving protonation states of amino acid side chains to be deduced in combination with other methods. Optical absorbance methods do have significant advantages in time resolution and signal-to-noise ratio for photolabile samples, so new intermediates along the photoexcitation pathway are usually first detected in optical absorbance studies.

Effect of E181 Mutations on Early Photointermediates. The most substantial perturbation of Batho decay kinetics occurred for the E181Q and E181F mutations. Similar accelerated Batho decay was originally seen in a number of artificial rhodopsins with synthetically modified retinal chromophores (*12*, *15*) and has been observed for several mutants of G121 (*13*). In general, modifications which reduce the barrier to rotation around the connection of the polyene chain to the β-ionone ring have been associated with fast Batho decay. It is interesting that the barrier is preserved in the E181D mutation, which is one carbon atom shorter than glutamic acid, while the barrier is substantially reduced for E181Q, which is a more isosteric substitution. This suggests that normal Batho stability requires a carboxyl property that cannot be substituted by glutamine at 181. While ionization is an obvious candidate, it is also possible that a hydrogen-bonding network could be disrupted by the different hydrogen-bonding character of glutamic acid's hydroxyl (one donor and two acceptors) and glutamine's amine (two donors and one acceptor) without invoking ionization of E181 as early as Batho.

Besides the kinetic perturbations of the Batho decay rate, the BSI λ_{max}'s are clearly affected by E181 mutation. A larger blue shift from the normal rhodopsin value (30 nm) is seen in E181D, which is consistent with the fact that the X-ray crystal structure predicts that E181D moves the carboxyl group toward the PSB end of the chromophore. An electrostatic map of the chromophore binding region (*16*) shows a nodal plane (where a charged group has no effect on the absorption spectrum) near the position of E181 in the crystal structure. Movement of a negatively charged group away from this plane toward the PSB end of the chromophore would blue shift the absorption spectrum. Increased interaction of the PSB with D181 at BSI as compared to E181 might account for the fact that a larger blue shift is seen for E181D BSI. The opposite behavior, a smaller shift compared to the shift seen in wild type, is seen for E181F and E181Q BSI's. It is interesting that the addition of chloride ion partially rescues this mutation-induced shift of the E181Q BSI spectrum.

Effect of E181 Mutations on Later Photointermediates. As might be expected from the similarity of E181D to wild-type rhodopsin on the submicrosecond time scale, E181D intermediate kinetics had more similarity to wild type than the other E181 mutants did at later times. The extra blue shift that characterized E181D BSI seems to persist into the E181D Lumi I spectrum, but E181D Lumi II seems to more closely approach the spectral shift found for Lumi II from bovine rhodopsin. Thus, if an increased interaction between the PSB and D181 is responsible for the increased blue shift of E181D BSI and E181D Lumi I, the constancy of Lumi II may indicate that the chromophore has reoriented the nodal plane so that aspartic acid or glutamic acid at position 181 have the same distance from it.

In contrast to E181D, which perturbs but does not grossly alter the rhodopsin intermediate scheme, E181F shows an extraordinarily early Schiff base deprotonation, in parallel with the formation of Lumi II. This unique behavior is not seen for the E181Q mutant. Almost certainly, the considerable difference in bulk of the glutamic acid and phenylalanine side chains accounts for some of the difference in Schiff base deprotonation rate. The destabilization of Batho in E181F suggests at least that the chromophore environment in the binding pocket is perturbed, and one cause of early deprotonation could be that the packing imperfection extends outward toward the aqueous phase, possibly admitting water more quickly. Disruption of the aqueous interface in E181F is supported by the observation that it has hydroxylamine reactivity orders of magnitude greater than rhodopsin (*17*). Further, the disruption of the pocket apparently does not cease with Lumi II formation since the E181F Meta II spectrum also appears to be blue shifted compared to that seen for wild-type rhodopsin.

The role of phenylalanine bulk in disrupting chromophore pocket packing is supported by data for the E181Q mutant. More isosteric glutamine at 181 shows no early PSB

deprotonation (compare the composition of sequential intermediate 4, Table 3) and has a Meta II absorbance which is almost 10 nm red shifted compared to that of E181F. This suggests that the hydrophobicity of the pocket is better preserved in E181Q, which has a 30-fold slower reactivity with hydroxylamine compared to E181F. The steric origin of the increased E181F pigment−hydroxylamine reactivity is supported by the fact that another isosteric, extracellular loop II mutant, D190N, similarly does not increase the rate of dark hydroxylamine attack (*18*). However, even for isosteric E181Q some aqueous accessibility to the binding pocket must be possible because chloride produces significant shifts in the E181Q pigment spectrum and in the spectra of E181Q intermediates, apparently blue shifting all except Lumi II. Another effect of added chloride on E181Q is to stabilize the PSB in the Lumi II/Meta I_{380} equilibrium (see Table 3). However, it remains to be determined whether the unusually fast deprotonation of the E181F Schiff base is purely due to phenylalanine's large side chain bulk or is also contributed to by its inability to even partially substitute for glutamic acid in a hydrogen-bonding network.

Electrostatic Effects in the Chromophore Binding Pocket. The primary determinant of the long-wavelength absorbance band of rhodopsin is the protonation of the *n*-retinylidene Schiff base, a condition guaranteed by the presence of the native counterion, glutamate at position 113. To a smaller degree, the rhodopsin absorbance maximum can be shifted by amino acid substitutions that change the polarity of residues near the chromophore. Such shifts, as their electrostatic origin implies, can be discussed in terms of the effect which would be introduced by a small test charge. Electrostatic models of retinal binding proteins (*19*, *20*) have shown that the direction of the absorbance shift depends on which end of the *n*-retinylidene chromophore the test charge approaches, with the smallest effect caused by a test charge that approaches the middle of the chromophore. From this standpoint, the retinal chromophore is poorly positioned to determine the ionization state of E181 since the X-ray crystal structure shows the E181 carboxyl to be positioned near the center of the chromophore, making the absorbance of rhodopsin relatively insensitive to E181's ionization state (*21*). Thus it is not surprising that absorbance measurements on rhodopsin mutants do not give a clear-cut answer about whether E181 is ionized in the dark.

The reported red shift of the rhodopsin spectrum induced by the E181Q mutation and its full (*1*) or partial (*4*) rescue by chloride suggest that E181 could be ionized. In agreement with this view, the E181D mutation blue shifts the pigment spectrum, an effect consistent with the picture of the E181 side chain from X-ray diffraction that implies the E181D mutation moves the carboxyl toward the protonated Schiff base. Further support for E181 ionization comes from a recent molecular dynamics simulation (*22*). Arguing against E181 ionization in rhodopsin is the fact that numerous other neutral mutations do not produce a red shift, including at least one (E181H) which blue shifts the pigment spectrum by as much as E181D. Beyond this specific evidence implying that E181 is neutral, there is the broader argument that if E181 is ionized in rhodopsin, it is not clear where compensating positive charge would come from to neutralize the binding site in the hydrophobic chromophore binding pocket. However, resting on hydrophobicity, the latter argument is not as certain as it once was. Besides showing that E181 is within about 5 Å of the chromophore, refinements of the rhodopsin crystal structure (*23*) have revealed the presence of a potentially extensive hydrogen-bonding network near the chromophore, including at least two water molecules, so the hydrophobicity of the environment near position 181 is not absolute. In addition to being polar, such a network of hydrogen bonds should be quite polarizable, and some mutations of E181 such as E181F versus E181Q could disrupt it more, reducing its polarizability. While polarizability is in some sense a second- or even third-order electrical phenomenon, in the case of a chain of hydrogen bonds near the rhodopsin chromophore, it is of primary importance because tautomerization of a sequence of hydrogen bonds could be the mechanistic basis of the counterion shift. Further studies will be required to determine to what degree mutations at position 181 act directly through a charge effect (e.g., E181F and E181Q ± chloride) versus their effect on polarizability (e.g., E181F).

Besides the polarity of residues in the chromophore binding pocket and polarizability of any hydrogen-bonding network intrinsic to the protein and bound water molecules, a final electrostatic effect that needs to be considered is that E181 is very near the aqueous interface. This is demonstrated by the fact that position 181 is analogous to one of the residues that forms the chloride binding site in LW2 cone visual pigments (*24*). The fact that the chloride binding affinity is affected by photolysis in one such cone pigment, P521 from gecko (*25*), demonstrates that the progress of the photoexcitation intermediates changes the electrical properties in this region. Hence, beyond the question of the relative significance of polarity and polarizability intrinsic to rhodopsin's hydrogen-bonding network in the progression of intermediates, external effects such as chloride ions and water penetration have to be considered. The possibility that chloride ion could bind to E181Q to mimic an ionized, but not titrable carboxyl (*26*) means that all experiments must be carefully evaluated for chloride effects.

In this context of effects external to rhodopsin, it is important to keep in mind that other factors besides mutations affect the rate of PSB deprotonation. Most detergents dramatically accelerate Schiff base deprotonation, but a few like digitonin seem to reduce the tendency to deprotonate and stabilize the late Meta I_{480} intermediate. Since rhodopsin mutants are typically purified in lauryl maltoside, which speeds up deprotonation by at least an order of magnitude, care must be taken in interpreting the effect of E181 mutations on activation. In particular, it is possible that detergent solubilization could affect the protonation state of E181 either in the dark or at one of the photointermediate states, masking a counterion shift which occurs in either membrane- or digitonin-solubilized preparations which support Meta I_{480} formation. It is clearly desirable to extend studies of the mutants characterized here in lauryl maltoside suspension to an environment that supports wild-type Meta I_{480}. However, even in the absence of such studies, the results presented here strongly support the idea that a negative charge at position 181 stabilizes protonation of the retinylidene Schiff base in the later intermediates. At the most elementary level this is demonstrated by the sequence of time constants observed for single-exponential fits of the late time data: WT > E181D > E181Q + Cl > E181Q − Cl >

E181F. It therefore seems possible that E181 may supply a counterion for an all-*trans* chromophore in the late photointermediates of vertebrate rhodopsins just as it does in the dark for invertebrate retinochrome.

REFERENCES

1. Terakita, A., Yamashita, T., and Shichida, Y. (2000) Highly conserved glutamic acid in the extracellular IV−V loop in rhodopsins acts as the counterion in retinochrome, a member of the rhodopsin family, *Proc. Natl. Acad. Sci. U.S.A. 97*, 14263−14267.
2. Palczewski, K., Kumasaka, T., Hori, T., Behnke, C. A., Motoshima, H., Fox, B. A., Le Trong, I., Teller, D. C., Okada, T., Stenkamp, R. E., Yamamoto, M., and Miyano, M. (2000) Crystal structure of rhodopsin: A G protein-coupled receptor, *Science 289*, 739−745.
3. Terakita, A., Koyanagi, M., Tsukamoto, H., Yamashita, T., Miyata, T., and Shichida, Y. (2004) Counterion displacement in the molecular evolution of the rhodopsin family, *Nat. Struct. Mol. Biol. 11*, 284−289.
4. Yan, E. C. Y., Kazmi, M. A., Ganim, Z., Hou, J.-M., Pan, D., Chang, B. S. W., Sakmar, T. P., and Mathies, R. A. (2003) Retinal counterion switch in the photoactivation of the G protein coupled receptor rhodopsin, *Proc. Natl. Acad. Sci U.S.A. 100*, 9262−9267.
5. Pan, D., Ganim, Z., Kim, J. E., Verhoeven, M. A., Lugtenburg, J., and Mathies, R. A. (2002) Time-resolved resonance Raman analysis of chromophore structural changes in the formation and decay of rhodopsin's BSI intermediate, *J. Am. Chem. Soc. 124*, 4857−4864.
6. Sakmar, T. P., Franke, R. R., and Khorana, H. G. (1989) Glutamic acid-113 serves as the retinylidene Schiff base counterion in bovine rhodopsin, *Proc. Natl. Acad. Sci. U.S.A. 86*, 8309−8313.
7. Fahmy, K., and Sakmar, T. P. (1993) Light-dependent transducin activation by an ultraviolet-absorbing rhodopsin mutant, *Biochemistry 32*, 9165−9171.
8. Zvyaga, T. A., Fahmy, K., and Sakmar, T. P. (1994) Characterization of rhodopsin-transducin interaction−a mutant rhodopsin photoproduct with a protonated schiff base activates transducin, *Biochemistry 33*, 9753−9761.
9. Lewis, J. W., and Kliger, D. S. (2000) Absorption spectroscopy in studies of visual pigments: Spectral and kinetic characterization of intermediates. *Methods Enzymol. 315*, 164−178.
10. Hug, S. J., Lewis, J. W., Einterz, C. M., Thorgeirsson, T. E., and Kliger, D. S. (1990) Nanosecond photolysis of rhodopsin: evidence for a new, blue-shifted intermediate, *Biochemistry 29*, 1475−1485.
11. Szundi, I., Lewis, J. W., and Kliger, D. S. (1997) Deriving reaction mechanisms from kinetic spectroscopy. Application to late rhodopsin intermediates, *Biophys. J. 73*, 688−702.
12. Randall, C. E., Lewis, J. W., Hug, S. J., Björling, S. C., Eisner-Shanas, I., Friedman, N., Ottolenghi, M., Sheves, M., and Kliger, D. S. (1991) A new photolysis intermediate in artificial and native visual pigments, *J. Am. Chem. Soc. 113*, 3473−3485.
13. Jäger, S., Han, M., Lewis, J. W., Szundi, I., Sakmar, T. P., and Kliger, D. S. (1997) Properties of early photolysis intermediates of rhodopsin are affected by glycine 121 and phenylalanine 261, *Biochemistry 36*, 11804−11810.
14. Szundi, I., Lewis, J. W., and Kliger, D. S. (2003) Two intermediates appear on the lumirhodopsin time scale after rhodopsin photoexcitation, *Biochemistry 42*, 5091−5098.
15. Mah, T. L., Lewis, J. W., Sheves, M., Ottolenghi, M., and Kliger, D. S. (1995) Low-temperature trapping of early photointermediates of alpha-isorhodopsin, *Photochem. Photobiol. 62*, 356−360.
16. Vought, B. W., Dukkipatti, A., Max, M., Knox, B. E., and Birge, R. R. (1999) Photochemistry of the primary event in short-wavelength visual opsins at low temperature, *Biochemistry 38*, 11287−11297.
17. Yan, E. C. Y., Kazmi, M. A., De, S., Chang, B. S. W., Seibert, C., Marin, E. P., Mathies, R. A., and Sakmar, T. P. (2002) Function of extracellular loop 2 in rhodopsin: Glutamic acid 181 modulates stability and absorption wavelength of metarhodopsin II, *Biochemistry 41*, 3620−3627.
18. Janz, J. M., Fay, J. F., and Farrens, D. L. (2003) Stability of dark state rhodopsin is mediated by a conserved ion pair in intradiscal loop E-2, *J. Biol. Chem. 278*, 16982−16991.
19. Birge, R. R., and Knox, B. E. (2003) Perspectives on the counterion switch-induced photoactivation of the G protein-coupled receptor rhodopsin, *Biochemistry 42*, 9105−9107.
20. Kusnetzow, A., Dukkipati, A., Babu, K. R., Singh, D., Vought, B. W., Knox, B. E., and Birge, R. R. (2001) The photobleaching sequence of a short-wavelength visual pigment, *Biochemistry 40*, 7832−7844.
21. Schreiber, M., Buss, V., and Sugihara, M. (2003) Exploring the Opsin shift with ab initio methods: Geometry and counterion effects on the electronic spectrum of retinal, *J. Chem. Phys. 119*, 12045−12048.
22. Röhrig, U. F., Guidoni, L., and Rothlisberger, U. (2002) Early steps of the intramolecular signal transduction in rhodopsin explored by molecular dynamics simulations, *Biochemistry 41*, 10799−10809.
23. Okada, T., Fujiyoshi, Y., Silow, M., Navarro, J., Landau, E. M., and Shichida, Y. (2002) Functional role of internal water molecules in rhodopsin revealed by X-ray crystallography, *Proc. Natl. Acad. Sci. U.S.A. 99*, 5982−5987.
24. Wang, Z. Y., Asenjo, A. B., and Oprian, D. D. (1993) Identification of the Cl^--binding site in the human red and green color vision pigments, *Biochemistry 32*, 2125−2130.
25. Lewis, J. W., Liang, J., Ebrey, T. G., Sheves, M., and Kliger, D. S. (1995) Chloride effect on the early photolysis intermediates of a gecko cone-type visual pigment, *Biochemistry 34*, 5817−5823.
26. Vogel, R., Fan, G. B., Siebert, F., and Sheves, M. (2001) Anions stabilize a metarhodopsin II-like photoproduct with a protonated Schiff base, *Biochemistry 40*, 13342−13352.
27. Mah, T., Szundi, I., Lewis, J. W., Jäger, S., and Kliger, D. S. (1998) The effects of octanol on the late photointermediates of rhodopsin, *Photochem. Photobiol. 68*, 762−770.
28. Jäger, S., Lewis, J. W., Zvyaga, T. A., Szundi, I., Sakmar, T. P., and Kliger, D. S. (1997) Time-resolved spectroscopy of the early photolysis intermediates of rhodopsin Schiff base counterion mutants, *Biochemistry 36*, 1999−2009.
29. Szundi, I., Mah, T. L., Lewis, J. W., Jäger, S., Ernst, O. P., Hofmann, K. P., and Kliger, D. S. (1998) Proton-transfer reactions linked to rhodopsin activation, *Biochemistry 37*, 14237−14244.

BI049581L